LANGMUIR

pubs.acs.org/Langmuir Article

Ecofriendly Microencapsulated Phase-Change Materials with Hybrid Core Materials for Thermal Energy Storage and Flame Retardancy

Zhong-Ting Hu,[#] Varghese Hansen Reinack,[#] Jinliang An, Zope Indraneel, Aravind Dasari, Jinglei Yang, and En-Hua Yang*

Cite This: *Langmuir* 2021, 37, 6380–6387 Read Online

ACCESS | Metrics & More | Article Recommendations | Supporting Information

ABSTRACT: Microencapsulated phase-change material (ME-PCM) employing octadecane as a core material has been practiced for thermal-energy-storage (TES) applications in buildings. However, octadecane as a hydrocarbon-based PCM is flammable. Herein, silica-shelled microcapsules (SiO_2-MCs) and poly(urea-formaldehyde)-shelled microcapsules (PUF-MCs) were successfully prepared, loaded with octadecane/tributyl phosphate (TBP) as hybrid core materials, which not only exhibited good TES properties but also high-effective flame retardancy. SiO_2-MC (ΔH_m = 124.6 J g^{-1} and ΔH_c = 124.1 J g^{-1}) showed weaker TES capacity than PUF-MC (ΔH_m = 186.8 J g^{-1}, ΔH_c = 188.5 J g^{-1}) but better flame retardancy with a lower peak heat-release rate (HRR_{peak}) of 460.9 W g^{-1} (556.9 W g^{-1} for PUF-MCs). As compared with octadecane (38.7 kJ g^{-1}), the reduction in total heat release (THR) for SiO_2-MC was up to 22% (30.1 kJ g^{-1}) with combustion time shortened by 1/6. SiO_2-MC had a typical diameter of 150−210 μm, shell thickness of ∼6.5 μm, and a core fraction of 84 wt %. SiO_2-MC showed better thermal stability with a higher initial evaporation/pyrolysis temperature than PUF-MC. The thermal decomposition of MCs with its mechanism of flame retardancy was significantly studied using thermogravimetric analysis/infrared spectrometry (TG-IR). The strategy presented in this study should inspire the development of microcapsules with PCMs/flame retardants as hybrid core materials for structural applications.

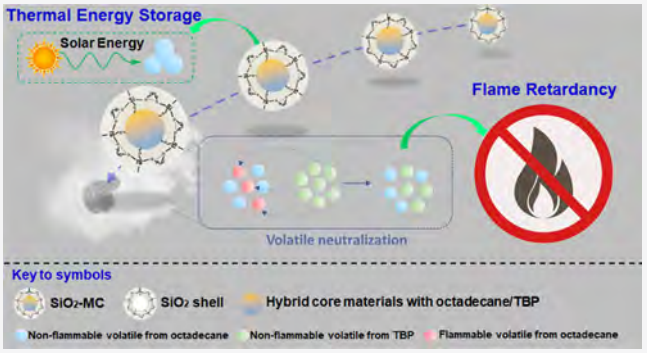

INTRODUCTION

Phase-change materials (PCM), known for their high thermal-energy-storage (TES) capacity via phase transition (e.g., solid−liquid), have been used to enhance thermal comfort of occupants and to reduce the energy consumption of buildings since 1980.[1−3] Building materials incorporating organic PCMs (e.g., octadecane) have been widely studied and applied in many applications. This is because organic PCMs possess high latent heat capacity, no subcooling, excellent thermal and chemical stability, no corrosion, and low cost.[4,5] However, one of the major disadvantages of organic PCMs is flammability, especially for hydrocarbon-based PCMs, as well as its environmental hazards.[6−8] Therefore, proper fire and environmental safety precautions are necessary when organic PCMs are incorporated into building materials.

Microencapsulation is a technique of enclosing microscaled organic PCM into a shell, which, in turn, isolates and protects PCM from the external environment.[6] The core/shell structure of microencapsulated phase-change material (ME-PCM) prevents leakage of liquefied PCM in the building materials. Various polymers, such as poly(methyl methacrylate) (PMMA)[9] and melamine-formaldehyde (MF),[10] were widely studied as shell materials of ME-PCM due to their good compatibility with a variety of PCMs. However, under elevated temperature, polymer shells decompose and even participate in combustion. Inorganic shell materials such as silicon dioxide (SiO_2), titanium dioxide (TiO_2), and aluminum oxide (Al_2O_3) may reduce total heat release, improve thermal stability, and enhance fire resistance of ME-PCM.[11−17] In general, inorganic shells performed worse than polymer shells in terms of avoiding penetration since inorganic shells are easy to crack toward pressure change caused by melt−freeze cycles. Therefore, it is insufficient to only rely on microencapsulation techniques for avoiding a fire.

The addition of flame retardants (FRs) to PCMs is one of the promising approaches to overcome PCM flammability.[18,19] FRs release radicals during thermal decomposition to inhibit combustion chain reactions. The nitrogen- or phosphorus-based FRs (namely, N-FRs or P-FRs) are halogen-free and more

Received: December 19, 2020
Revised: March 9, 2021
Published: May 17, 2021

https://doi.org/10.1021/acs.langmuir.0c03587
Langmuir 2021, 37, 6380−6387

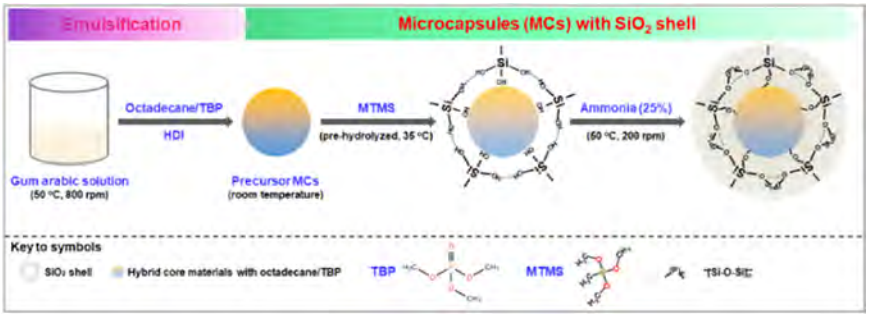

Figure 1. Schematic illustration of formation of microcapsules with a silica shell and an octadecane/TBP hybrid core.

Table 1. Thermophysical Properties of As-Prepared ME-PCMs Based on the Enthalpy Change and Burning Heat Release

sample	core material (octadecane/TBP ratio)	shell material	ΔH_m[b] (J g^{-1})	ΔH_c[c] (J g^{-1})	THR[d] (kJ g^{-1})	HRR_{peak}[e] (W g^{-1})
octadecane			228.4	228.7	38.7	629.6
SiO_2-MC1	1/0	SiO_2	169.3	171.8	37.5	455.6
SiO_2-MC2	19/1	SiO_2	173.4	175.4	36.4	577.8
SiO_2-MC3	9/1	SiO_2	168.7	173	34.5	573.5
SiO_2-MC	4/1	SiO_2	124.6	124.1	30.2	460.9
PUF-MC	4/1	PUF	186.8	188.5	30.1	556.9
[a] TBP[a]					24.6	528

[a]Tributyl phosphate. [b]Enthalpy change of a microcapsule in the melting process. [c]Enthalpy change of a microcapsule in the crystallization process. [d]Total heat release. [e]Peak heat-release rate.

environmentally friendly.[20−23] In particular, the phosphorus-based radicals are 10 times more effective than the •Cl and 5 times better chain terminator than •Br.[7,24] It has been reported that the P-FRs (e.g., commercial ammonium polyphosphate, APP) can act in both the gas and the condensed phases during a fire as a result of its chemical versatility.[25,26] As Wirasaputra et al. reported in a fire test of polymeric materials, 9,10-dihydro-9-oxa-10-phosphaphenanthrene-10-oxide (DOPO)-triazine based anhydride (2,4,6-tris-(DOPO-methylformatephthalic anhydride-phenoxy)-1,3,5-triazine (TDA)) was prepared and successfully acted as a flame retardant for diglycidyl ether of a bisphenol A/methylhexahydrophthalic anhydride (DGEBA/MHHPA) system via the formation of char and vaporized water.[27] Meanwhile, in the mode of gas-phase action, Yang et al. fabricated a novel halogen-free flame retardant (namely, DTB) and demonstrated that free radicals (e.g., •PO and •PO_2) were generated from DTB to react with •H (or •HO) radicals formed in chain reactions of epoxy resin during conditional combustion.[28]

In this study, TBP was used as a halogen-free FR and added into octadecane PCM to form a hybrid core material. PCM/TBP microcapsules with either a SiO_2 shell or a poly(urea-formaldehyde) (PUF) shell were synthesized. The resulting SiO_2-shelled microcapsules (SiO_2-MC) and PUF-shelled microcapsules (PUF-MC) were characterized and the thermal properties and combustion behavior were investigated and compared. The combustion of SiO_2-MC and PUF-MC was carried out by means of pyrolysis combustion flow calorimetry (PCFC) and TG-IR. Important parameters evaluating the fire hazard, including the total heat release (THR), the peak heat-release rate (HRR_{peak}), and the combustion time (t_c), were studied and discussed.

EXPERIMENTAL SECTION

Materials. Octadecane (99%), tributyl phosphate (TBP, 99%), gum arabic, methyltrimethoxysilane (MTMS, 98%), urea, ammonium chloride, ammonia (25%), resorcinol, sodium hydroxide, hydrochloric acid, and formaldehyde (37 wt % aqueous solution) were purchased from Sigma-Aldrich. Hexamethylene diisocyanate (HDI, 99%) was sourced from Huntsman Polyurethanes. Ethylene maleic anhydride (EMA) copolymer was obtained from MP Biomedicals. All of the chemicals used in this study were used as purchased without further purification.

Synthesis of Silica-Shelled Microcapsules (SiO_2-MCs). SiO_2-shelled microcapsules were prepared using a facile method at low temperature, which is modified from our previous study.[29] Typically, 0.93 g of gum arabic was dissolved in 30 mL of DI water at room temperature. The solution was agitated at 800 rpm and heated to 50 °C at a rate of 5 °C min^{-1}. Five grams of core materials (mixture of octadecane/TBP with a certain ratio) and 1 g of HDI were added into the solution followed by formation of an emulsion. The emulsion was agitated for 3 h; after that the reaction temperature was naturally cooled to room temperature. The precursor microcapsules formed were washed in DI water thrice followed by resuspension in 50 mL of water at 200 rpm. Two grams of MTMS was hydrolyzed in 4 g of HCl (pH ∼ 3) at 35 °C for 1 h. The hydrolyzed MTMS was added dropwise to the precursor microcapsules followed by addition of an ammonia solution (25%) at 50 °C. After 24 h, the obtained microcapsules were filtered, washed, and dried in air. The synthesis procedure is schematically illustrated in Figure 1, and the as-prepared samples were denoted as SiO_2-MC1, SiO_2-MC2, SiO_2-MC3, and SiO_2-MC based on different octadecane/TBP ratios (Table 1).

Synthesis of Poly(urea-formaldehyde)-Shelled Microcapsules (PUF-MCs). PUF-shelled microcapsules were prepared by simplified in situ polymerization in an oil-in-water emulsion.[30] At a constant temperature (35 °C), 40 mL of deionized water and 10 mL of a 2.5 wt % EMA aqueous solution were added to a 200 mL beaker. The beaker was suspended in a temperature-controlled water bath on a programmable hotplate with an external temperature probe. The solution was agitated with a three-bladed mechanical stirrer. Urea (1.0 g), ammonium chloride (0.1 g), and resorcinol (0.1 g) were dissolved in the solution under agitation at 800 rpm. The pH of the solution was adjusted at 3.0 by dropwise addition of sodium hydroxide and hydrochloric acid. Core materials (10 g) with the octadecane/TBP ratio of 4/1 was added into the mixture solution to form an emulsion and allowed to stabilize for 10 min. After stabilization, 2.53 g of a 37 wt % aqueous solution of formaldehyde was added dropwise. The emulsion was covered with an alumina paper and heated at a rate of

https://doi.org/10.1021/acs.langmuir.0c03587
Langmuir 2021, 37, 6380−6387

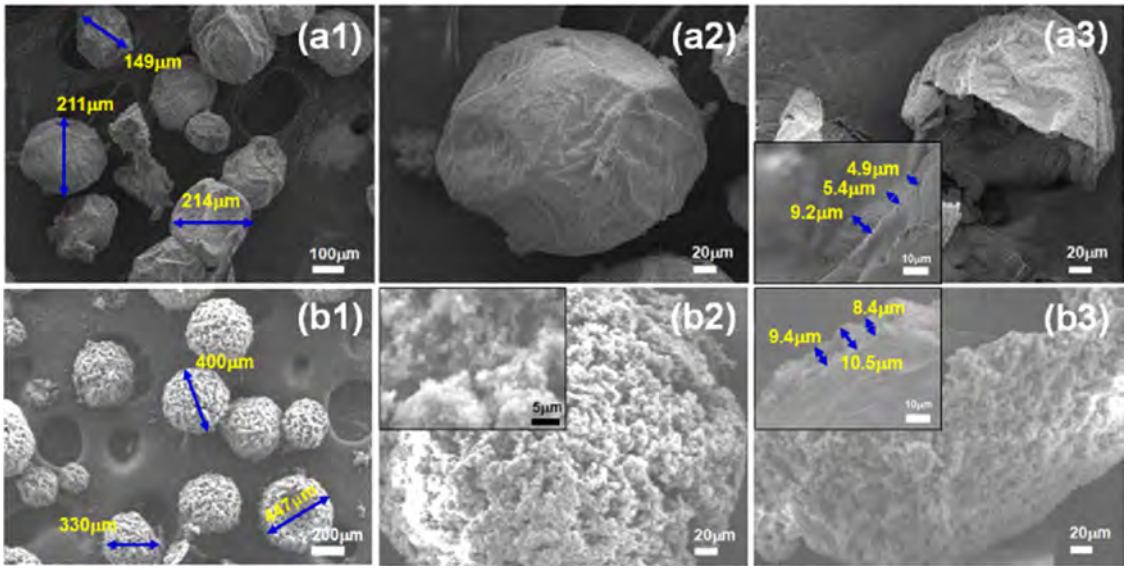

Figure 2. SEM images of hybrid ME-PCMs with different shell materials of SiO_2 (a1−a3, denoted SiO_2-MC) and PUF (b1−b3, denoted PUF-MC).

1 °C min^{-1} to the target temperature of 55 °C. After 4 h of continuous agitation at 200 rpm, the stirrer and the hotplate were switched off. Once the system was cooled to ambient temperature, the suspension of microcapsules was separated under vacuum with a coarse-fritted filter. The final microcapsules were rinsed with DI water and dried in a fume hood for 24 h prior to use. The as-prepared samples were denoted as PUF-MC listed in Table 1.

Characterization. Surface morphology of the microcapsules was observed using scanning electron microscopy (SEM, JEOL JSM-7600F). The elemental composition of the microcapsules was examined by X-ray energy-dispersive spectroscopy (EDS, JOEL JSM-7600F). The as-prepared microcapsules were analyzed using Fourier transform-infrared spectroscopy (FT-IR, PerkinElmer Frontier) to characterize the constituents of the microcapsules. The thermal stability property and component fractions of the as-prepared microcapsules were investigated by thermogravimetric analysis (TGA, PerkinElmer TGA4000). For the TGA test, approximately 10 mg of the samples was put into an alumina crucible and heated under a nitrogen atmosphere from 30 to 500 °C at a rate of 10 °C min^{-1}. The volatile compounds and/or gas-phase byproducts released from microcapsules in controlled processes of temperature and the N_2 atmosphere were measured using thermogravimetry-infrared spectroscopy (TG-IR) coupled analysis (PerkinElmer TGA4000 and PerkinElmer Frontier FT-IR). Moreover, the thermal properties of the as-prepared microcapsules were characterized using differential scanning calorimetry (DSC, TA Instruments DSC Q10) from −20 to 50 °C at a ramp rate of 10 °C min^{-1}. Heat release of samples at a fixed mass was measured using an FAA Micro Calorimeter from Quantum Technologies Global Pte Ltd, Singapore.

RESULTS AND DISCUSSION

Synthesis and Characteristics of the As-Prepared Microcapsules. SiO_2-MCs were successfully fabricated using a facile method at a low temperature (Figure 1), while PUF-MCs were synthesized through in situ polymerization in an oil-in-water emulsion at 55 °C. Spherical SiO_2-MC with a diameter of 150−210 μm was obtained, as shown in Figure 2a1, whereas PUF-MC has a larger diameter of 330−447 μm (Figure 2b1) at a similar agitation rate. The obvious alteration of the microcapsule size is ascribed to the effects of relative viscosity[31] and interfacial tension[32] between the dispersed and continuous phases in the whole system of microcapsule (MC) synthesis. It implies that PUF-MC preparation via in situ polymerization processes showed a higher relative viscosity than that of SiO_2-MC. Moreover, the increasing size of SiO_2-MCs with the increasing portion of TBP in the mixture of octadecane/TBP (from the ratios of 1/0, 19/1, and 9/1 to 4/1) indicated that the partial hydrolysis of TBP with a −OH functional group is capable of reducing the interfacial tension between the core and continuous phase (Figures S1a−c and 2a). As compared with SiO_2-MC1 (no detected phosphorus), the EDX spectrum of SiO_2-MC shows the characteristic peaks of silicon, oxygen, and phosphorus, respectively (Figure S2). This phenomenon is plausibly indicated by the following aspects: (1) there is a possibility of introducing TBP into the SiO_2 shell and (2) it is reasonable to believe that TBP has been successfully encapsulated into SiO_2-MCs. Furthermore, the scanning electron microscopy (SEM) images at a higher magnification showed the different surface structures for the as-prepared MCs significantly (Figure 2a2,b2). SiO_2-MC displayed a smooth structure with wrinkles on the surface, while PUF-MC showed a hierarchical outer surface structure like a lotus leaf surface (inset of Figure 2b). This hierarchical structure on the surface of PUF-MC is attributed to the spontaneous deposition of poly(urea-formaldehyde) (PUF) nanoparticles as the polymerization reaction progresses.[30] It is obvious that the microcapsules have a core−shell structure for both SiO_2-MC (Figure 2a3) and PUF-MC (Figure 2b3) with average shell thicknesses of ∼6.5 and ∼9.4 μm, respectively, which implies that encapsulation conditions used were successful in forming capsules.

Figure 3 shows the FT-IR spectra of pure octadecane, pure TBP, SiO_2-MC, and PUF-MC. The characteristic peaks of both in octadecane and TBP are attributed to the hydrocarbon chain in their molecular structures. The peaks at approximately 2926, 2857, 1471, 1374, and 722 cm^{-1} are assigned to C−H stretching in $-CH_3$, C−H stretching in $-CH_2-$, C−H bending in $-CH_2-$, C−H bending in $-CH_3$, and $-CH_2-$ in-plane rocking, respectively.[33−35] It is obvious that these characteristic peaks appeared both in SiO_2-MC and PUF-MC, thereby suggesting that octadecane/TBP as a core material has been successfully encapsulated into MCs. Moreover, additional vibrational modes of TBP, i.e., ν(TBP), detected at around 1273 and 1033 cm^{-1} in TBP, PUF-MC, and SiO_2-MC, are for vibration modes of P═O and stretching modes of C−O−P, respectively.[36,37] With the increase in the ratio of octadecane to TBP in SiO_2-MCs, it is

https://doi.org/10.1021/acs.langmuir.0c03587
Langmuir 2021, 37, 6380−6387

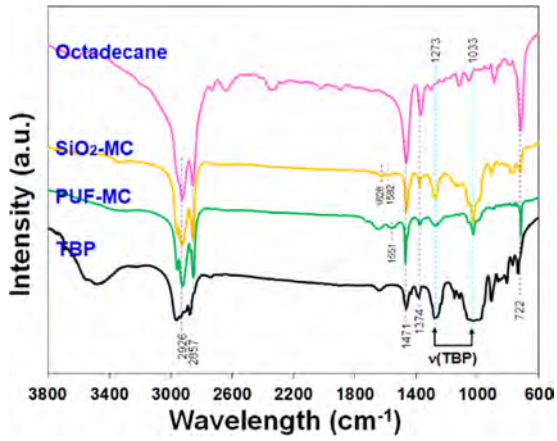

Figure 3. FT-IR transmittance spectra of octadecane, TBP, and as-prepared hybrid ME-PCMs (SiO_2-MC and PUF-MC) in 600−3800 cm^{-1}.

worth noticing that the signal of v(TBP) becomes weaker (Figure S3). This again suggests that MCs have been successfully prepared with encapsulating octadecane and TBP as hybrid core materials in a SiO_2 (or PUF) shell. In addition, the characteristic peaks at 1628 and 1582 cm^{-1} are ascribed to asymmetric Si−O−Si stretching vibrations of the SiO_2 compound (yellow curve in Figures 3 and S3), while the signal peak at 1551 cm^{-1} observed in the PUF compound is attributed to the carbonyl stretching vibration (green curve in Figure 3).[29,38]

Thermal Stability of Microcapsules. The mass loss profiles of SiO_2-MC and PUF-MC were obtained using thermogravimetric analysis (TGA). As shown in Figure 4, the

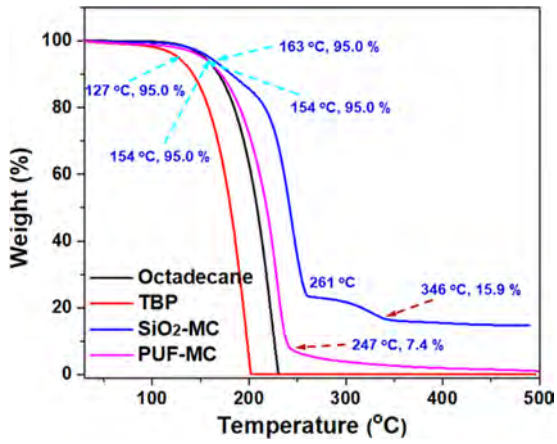

Figure 4. TGA curves of octadecane, TBP, SiO_2-MC, and PUF-MC under a N_2 atmosphere at a ramp rate of 10 °C min^{-1}.

TGA profiles for octadecane and TBP exhibited pyrolysis processes in a one-step model. The corresponding mass loss is 100% at 231 and 201 °C, respectively. For SiO_2-MC, a two-step model is seen, where ∼75% mass loss occurs by 261 °C and another ∼10% by 346 °C. For PUF-MC, ∼92.6% is lost by 247 °C. This indicates that MCs possessed better thermal stability. At an even higher temperature beyond 400°C, PUF-MC showed a complete weight loss while SiO_2-MC had a residual weight of 15% due to the presence of an inorganic SiO_2 shell. SiO_2-MC showed a higher initial evaporation temperature at 163 °C (defined as 5% weight loss) than that of TBP (127 °C) and octadecane (154 °C), indicating that octadecane/TBP as core materials encapsulated in a SiO_2 shell became more stable. Subsequently, the temperature for primary weight loss, which is mainly attributed to the evaporation/pyrolysis of the core material (octadecane and TBP), shifted to ∼261 °C (TGA curve of SiO_2-MC in Figure 4). This may be attributed to the protection from the SiO_2 shell and the presence of TBP in the core. As shown in the inset of Figure S4, the temperature for primary weight loss of SiO_2-MCs increases with increasing the TBP/octadecane ratio perhaps due to the flame retardancy property of TBP, which is in good agreement with the published literature.[11,18,39] Overall, it was found that the SiO_2 shell and the presence of TBP effectively improved the thermal stability of the octadecane core.

Thermal Energy Storage of Microcapsules. Thermophysical properties of as-prepared SiO_2-MCs and PUF-MCs based on the enthalpy change and melting/solidifying temperature in the melting/crystallization process were characterized using a differential scanning calorimeter (DSC).[3] As shown in Figure 5, the melting temperature of pure octadecane was in the

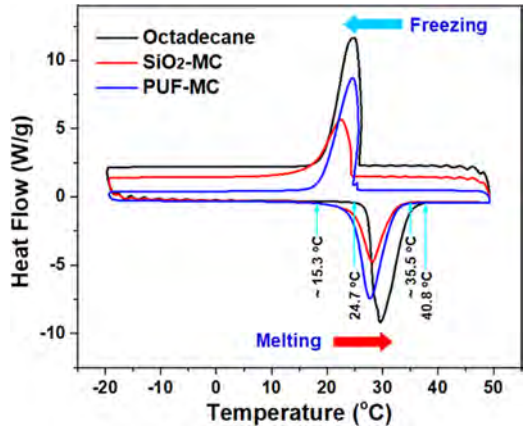

Figure 5. DSC curves of octadecane, SiO_2-MC, and PUF-MC at a rate of 10 °C min^{-1}.

range of 24.7−40.8 °C, while that of as-prepared MCs (i.e., SiO_2-MC and PUF-MC) shifted to ∼15.3−35.5 °C simultaneously. This suggests the melting process of MCs completes at lower temperatures than that of pure octadecane (∼9.4 and 5.3 °C early in the onset and the end melting process, respectively), which indicates the efficient thermal response of MCs (namely, good energy-storage efficiency) is achieved due to the large surface area after microencapsulation and is in good agreement with the published literature.[30] Correspondingly, the freezing process starts and ends later (e.g., ∼1.3 and 8 °C delay in the onset and the end freezing process for SiO_2-MC), as shown in Table 2.

Moreover, the peak positions of DSC curves on SiO_2-MC and PUF-MC have a slight alteration (Table 2), while the enthalpy change in the melting process (or the crystallization process) for SiO_2-MC and PUF-MC is ΔH_m of 124.6 J g^{-1} (ΔH_c of 124.1 J g^{-1}) and ΔH_m of 186.8 J g^{-1} (ΔH_c of 188.5 J g^{-1}), respectively (Table 1). It is obvious that PUF-MC has higher thermal-energy-storage (TES) capacity as compared to SiO_2-MC because PUF-MC contains more core material (core fractions of PUF-MC and SiO_2-MC are about 93 and 84 wt %, respectively).

Furthermore, the TES properties of MCs are influenced directly by the composition of core materials, which is possibly

https://doi.org/10.1021/acs.langmuir.0c03587
Langmuir 2021, 37, 6380−6387

Table 2. Phase-Change Characteristics of As-Prepared ME-PCMs Based on DSC Results

	melting process (°C)			freezing process (°C)		
sample	onset (T_{mo})[a]	peak (T_{mp})[b]	end (T_{me})[c]	onset (T_{co})[d]	peak (T_{cp})[e]	end (T_{ce})[f]
octadecane	24.7	29.7	40.8	25.8	24.8	16.1
SiO_2-MC1	21.1	30.2	39.2	25.5	23.9	14.7
SiO_2-MC2	21.2	30.3	39.3	25.3	23.4	12.9
SiO_2-MC3	18.4	29.5	39.4	25.0	22.9	12.1
SiO_2-MC	15.4	28.1	36.2	24.5	22.4	8.1
PUF-MC1[g]	22.6	29.2	38.3	26.1	25.0	15.8
PUF-MC2[h]	21.1	28.4	35.8	26.0	24.7	15.7
PUF-MC	15.2	27.9	34.8	25.6	24.5	15.0

[a]Onset temperature in the melting process. [b]Peak temperature in the melting process. [c]End temperature in the melting process. [d]Onset temperature in the freezing process. [e]Peak temperature in the freezing process. [f]End temperature in the freezing process. [g]Octadecane/TBP ratio is 1/0. [h]Octadecane/TBP ratio is 9/1.

ascribed to TBP in a liquid phase. The experimental results (Figures S5 and S6, Tables 1 and 2) basically demonstrated the following aspects: (1) The TES capacities of the MCs are inversely proportional to the increase in the TBP/octadecane ratio. The enthalpy value (ΔH_c) of SiO_2-MC1 with the octadecane/TBP ratio of 1/0 is 171.8 J g^{-1}, while SiO_2-MC with the octadecane/TBP ratio of 4/1 has a ΔH_c value of only 124.1 J g^{-1} only (Table 1, Figure S5). As shown in Figure S6, the peak value of PUF-MCs decreased in the order PUF-MC1 (octadecane/TBP of 1/0) > PUF-MC2 (octadecane/TBP of 9/1) > PUF-MC (octadecane/TBP of 4/1). (2) Overall, TES charging/discharging for MCs shifts to lower temperatures, especially for SiO_2-MC and PUF-MC with the octadecane/TBP ratio of 4/1 (Table 2). Moreover, the thermal property of SiO_2-MC shows a good performance after 1000 charging/discharging cycles (Figure S7, Tables S1 and S2).

Combustion Behavior of Microcapsules. Flammability of the microencapsulated phase-change material (ME-PCM) is one of the most important factors that has restricted its application especially in building applications.[7] As shown in Figure 6, the pyrolysis combustion flow calorimetry (PCFC) as a quantitative technique for assessing the flammability of octadecane, TBP, SiO_2-MC, and PUF-MC was investigated, respectively. The corresponding heat-release characteristics derived from PCFC tests including total heat release (THR) and peak heat-release rate (HRR_{peak}) are presented in Table 1. As evident, HRR_{peak} for octadecane, PUF-MC, and SiO_2-MC are in the order 629.6 > 556.9 > 460.9 W g^{-1}. HRR_{peak} reduction for SiO_2-MC reached 26.7% that is better than PUF-MC (11.5%). According to the experimental result, two conclusions could be extracted as follows: (1) TBP could effectively reduce HRR_{peak} of octadecane because TBP is one of the phosphorus-based fire retardants[7] and (2) the shell composed of inorganic materials (i.e., SiO_2) is more beneficial for HRR_{peak} reduction than that of organic compounds (i.e., PUF). A reliable reason for conclusion (2) is PUF combustion with heat release additionally. As shown in Table 1, THR is 38.7 and 24.6 kJ g^{-1} for octadecane and TBP, respectively. For the core material with the octadecane/TBP ratio of 4/1, the obtained THR for SiO_2-MC and PUF-MC is 30.2 and 30.1 kJ g^{-1}, respectively. In addition, THR for varied SiO_2-MCs can be adjusted from 37.5 kJ g^{-1} (SiO_2-MC1 with the ratio of 1/0) to 30.2 kJ g^{-1} (SiO_2-MC with the ratio of 4/1) through alteration of the octadecane/TBP ratio. Therefore, introduction of TBP into ME-PCM is an effective strategy for inhibiting combustion of flammable phase-change materials, in which a plausible mechanism is ascribed to phosphorus-based radicals (e.g., $^{\bullet}PO$ and $^{\bullet}PO_2$) functioning for the elimination of $^{\bullet}H$ (or $^{\bullet}HO$) radicals and termination of chain reactions.[40−42]

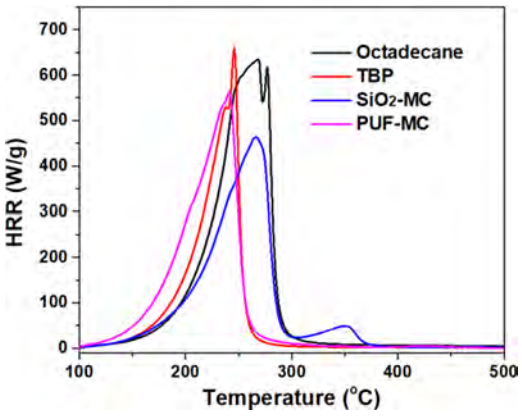

Figure 6. Flammability testing for octadecane, TBP, SiO_2-MC, and PUF-MC using pyrolysis combustion flow calorimetry (PCFC).

Thermal Decomposition of Microcapsules. Gaseous products (e.g., pyrolyzate), which directly relate to characteristics in pyrolysis, combustion, heat release, and/or smoke toxicity in a fire,[43,44] were detected using TG-IR for octadecane, TBP, SiO_2-MC, and PUF-MC from 30 to 500 °C (Figure 7). As shown in Figure 7a, it can be seen that the evolved gaseous products for octadecane show a characteristic peak at ∼3100 cm^{-1}, which might be synergistically assigned to the C−H stretching in $-CH_3$ (∼2960 cm^{-1}), =C−H absorbance (∼3010−3040 cm^{-1}), and C−H stretching in ≡CH (∼3300 cm^{-1}).[45,46] The corresponding absorption area is from ∼155 to ∼445 °C, wherein reaching the maximum intensity (I_{max}) of gas emission at ∼254 °C. A reasonable conclusion is that the evolved gaseous products from decomposition of octadecane are mainly composed of flammable alkanes, alkenes, and alkynes, in which octadecane ($CH_3(CH_2)_{16}CH_3$) attacked by $^{\bullet}H$ radicals broke into shorter hydrocarbon compounds (Figure 8, pyrolysis reactions 1−2 of alkanes). The evolved gaseous products (Figure 7b) for TBP ($C_{12}H_{27}O_4P$ with functional groups of $-O(CH_2)_3CH_4$) exhibited characteristic peaks at ∼3000, ∼1750, and ∼1350 cm^{-1}, which is possibly ascribed to the synergistic effect of the C−H stretching in $-CH_3$ (∼2960 cm^{-1}) and =C−H absorbance (∼3010−3040 cm^{-1}), C=O stretching, and C−H bending in CH_3, respectively.[44] ν(TBP) was not detected like it was observed above in Figure 3, indicating that TBP is easy to be decomposed in thermal treatment and it is plausibly transformed to phosphorus-based radicals and nonflammable gaseous products (e.g., H_2O).[26] The nonflammable gaseous products, which played an important role in a mechanism of fire retardancy, were used to dilute the flammable gaseous products evolved from octadecane (Figure 8).

In contrast, the characteristic peak of the evolved gaseous products was observed at 3050 cm^{-1} (I_{max} individually appeared at 173 and 250 °C) for SiO_2-MC (Figure 7c) and at 3030 cm^{-1} (I_{max} appeared at 205 °C) for PUF-MC (Figure 7d) with the C−N stretching at ∼1000 cm^{-1}. The position of the major characteristic peak for above mentioned MCs is simultaneously assigned to the C−H stretching in $-CH_3$ (∼2960 cm^{-1}) and =C−H absorbance (∼3010−3040 cm^{-1}). There was no detected C−H stretching in ≡ CH (∼3300 cm^{-1}), implying that alkynes

https://doi.org/10.1021/acs.langmuir.0c03587
Langmuir 2021, 37, 6380−6387

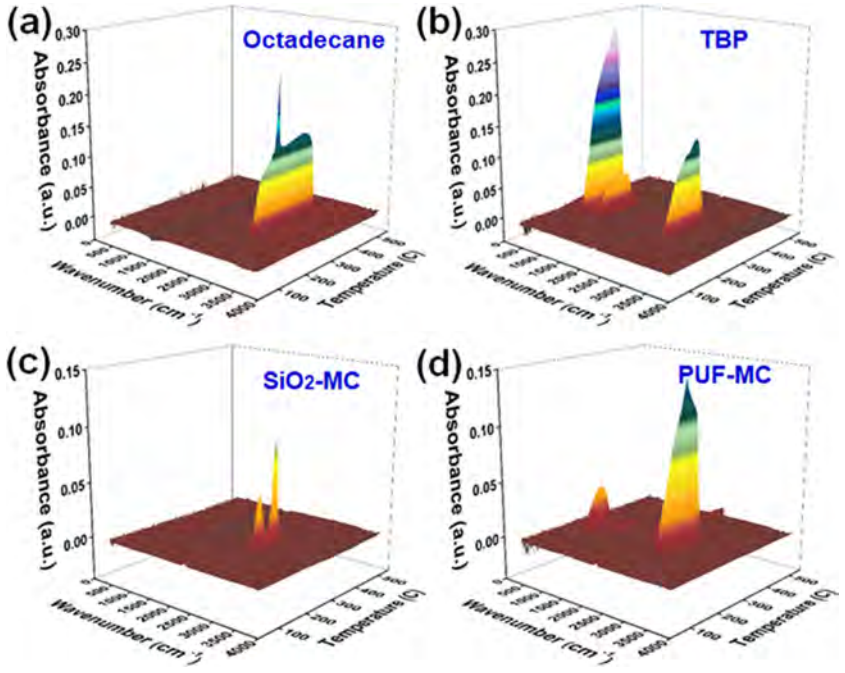

Figure 7. TG-IR spectra of octadecane (a), TBP (b), SiO_2-MC (c), and PUF-MC (d) under a N_2 atmosphere.

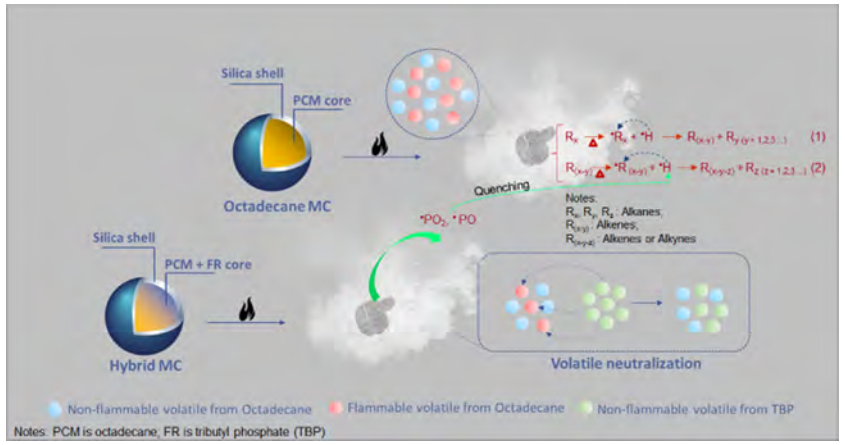

Figure 8. Schematic illustration of the flame retardant behavior of octadecane/TBP hybrid microencapsulated phase-change materials (ME-PCMs).

did not form with the termination of chain reactions of pyrolysis reaction 2. This result reflected another plausible mechanism, which is that the formed •H radicals were quenched by phosphorus-based radicals (Figure 8). In addition, it is worth noting that I_{max} of gaseous products for SiO_2-MC became much lower than that of pure octadecane, as well as the corresponding absorption area became narrower from ~125 to ~270 °C (Figure 7c), significantly meaning combustion with a short time and less gaseous products. A summary of T_o, T_e, P_{peak}, I_{max}, and t_c for the thermal decomposition of samples using TG-IR is presented in Table 3.

CONCLUSIONS

A microencapsulated phase-change material (ME-PCM) associated individually with polymeric (i.e., PUF-MC) and inorganic (i.e., SiO_2-MC) shell has been successfully synthesized using varied facile methods. The microcapsules (MCs) containing hybrid core materials of octadecane/TBP have excellent thermal properties and high-effective flame retardancy. Overall, compared with PUF-MC, SiO_2-MC exhibits better flame retardancy in terms of total heat release (THR), peak heat-release rate (HRR_{peak}), and combustion time (t_c) because the polymeric shell can contribute to combustion. Moreover, SiO_2-MC shows better thermal stability such as higher evaporation/

Table 3. TG-IR Analysis of Octadecane, TBP, SiO_2-MC, and PUF-MC

sample	T_o[a] (°C)	T_e[b] (°C)	$T_e - T_o$ (°C)	P_{peak}[c] (cm^{-1})	I_{max}[d] (°C)	t_c[e] (min)
octadecane	155	445	290	3100	250	30
TBP	150	310	160	3000	250	
135	260	125	1750	206		
135	305	170	1350	245		
SiO_2-MC	125	270	165	3030	173/ 250	5
PUF-MC	130	300	170	3010	205	
140	250	110	1000	160		

[a]Onset temperature. [b]End temperature. [c]Characteristic peak position. [d]Temperature appeared at the maximum intensity for the absorbance peak. [e]Combustion time.

https://doi.org/10.1021/acs.langmuir.0c03587
Langmuir 2021, 37, 6380−6387

pyrolysis temperatures with good thermal energy storage (TES) of ΔH_m of 124.6 J g^{-1}. Although the structure of microencapsulation can promote fire retardancy, the flame retardant TBP plays an initial role in flame retardancy. The obtained results show that the ratio of octadecane/TBP affects the fluctuation of flame retardancy, wherein the plausible mechanisms are ascribed to TBP releasing nonflammable gaseous products (e.g., moisture) and phosphorus-based radicals. The findings reveal the great potential for the strategy of encapsulating PCMs/flame retardants as hybrid core materials in an inorganic shell in the prevention and control of fire in buildings, as well as ensuring environmental sustainability.

■ ASSOCIATED CONTENT

Supporting Information

The Supporting Information is available free of charge at https://pubs.acs.org/doi/10.1021/acs.langmuir.0c03587.

SEM images of SiO_2-MC1, SiO_2-MC2, and SiO_2-MC3 with octadecane/TBP ratio of 1/0, 19/1, and 9/1 respectively; EDX spectra of SiO_2-MC1 and SiO_2-MC with octadecane/TBP ratio of 1/0 and 4/1 respectively (the selected microcapsules with cracks); TGA curves of octadecane, TBP, SiO_2-MC1, SiO_2-MC2, SiO_2-MC3, and SiO_2-MC; DSC curves of octadecane, SiO_2-MC1, SiO_2-MC2, SiO_2-MC3, and SiO_2-MC; DSC curves of SiO_2-MC at different charging/discharging cycles; SiO_2-MC performance on charging/discharging cycles; and comparison between SiO_2-MC and commercial products on performance of charging/discharging cycles (PDF)

■ AUTHOR INFORMATION

Corresponding Author

En-Hua Yang − *School of Civil and Environmental Engineering, Nanyang Technological University (NTU), 639798, Singapore;* orcid.org/0000-0001-6066-8254; Email: ehyang@ntu.edu.sg

Authors

Zhong-Ting Hu − *College of Environment, Zhejiang University of Technology, Hangzhou 310014, China;* orcid.org/0000-0003-3963-2104

Varghese Hansen Reinack − *School of Civil and Environmental Engineering, Nanyang Technological University (NTU), 639798, Singapore;* orcid.org/0000-0002-3582-6334

Jinliang An − *School of Civil Engineering, Hebei University of Engineering, Handan 056038, China*

Zope Indraneel − *School of Material Science and Engineering, NTU, 639798, Singapore*

Aravind Dasari − *School of Material Science and Engineering, NTU, 639798, Singapore;* orcid.org/0000-0003-0647-8577

Jinglei Yang − *Department of Mechanical and Aerospace Engineering, Hong Kong University of Science and Technology, Hong Kong, China;* orcid.org/0000-0002-9413-9016

Complete contact information is available at: https://pubs.acs.org/10.1021/acs.langmuir.0c03587

Author Contributions

#Z.-T.H. and V.H.R. are co-first authors.

Notes

The authors declare no competing financial interest.

■ ACKNOWLEDGMENTS

The authors would like to acknowledge financial support from the Agency for Science, Technology and Research (A*STAR)—Ministry of National Development (MND), Singapore (SERC132 176 0014).

■ REFERENCES

(1) Cabeza, L. F.; Castell, A.; Barreneche, C.; de Gracia, A.; Fernández, A. I. Materials used as PCM in thermal energy storage in buildings: A review. *Renewable Sustainable Energy Rev.* **2011**, *15*, 1675−1695.

(2) Bland, A.; Khzouz, M.; Statheros, T.; Gkanas, E. PCMs for residential building applications: A short review focused on disadvantages and proposals for future development. *Buildings* **2017**, *7*, 78.

(3) Safari, A.; Saidur, R.; Sulaiman, F. A.; Xu, Y.; Dong, J. A review on supercooling of phase change materials in thermal energy storage systems. *Renewable Sustainable Energy Rev.* **2017**, *70*, 905−919.

(4) Sharma, A.; Tyagi, V. V.; Chen, C. R.; Buddhi, D. Review on thermal energy storage with phase change materials and applications. *Renewable Sustainable Energy Rev.* **2009**, *13*, 318−345.

(5) Sharma, R. K.; Ganesan, P.; Tyagi, V. V.; Metselaar, H. S. C.; Sandaran, S. C. Developments in organic solid−liquid phase change materials and their applications in thermal energy storage. *Energy Convers. Manage.* **2015**, *95*, 193−228.

(6) Giro-Paloma, J.; Martínez, M.; Cabeza, L. F.; Fernández, A. I. Types, methods, techniques, and applications for microencapsulated phase change materials (MPCM): A review. *Renewable Sustainable Energy Rev.* **2016**, *53*, 1059−1075.

(7) Chandel, S. S.; Agarwal, T. Review of current state of research on energy storage, toxicity, health hazards and commercialization of phase changing materials. *Renewable Sustainable Energy Rev.* **2017**, *67*, 581−596.

(8) Ding, Y.; Zhao, J.; Liu, J.-W.; Zhou, J.; Cheng, L.; Zhao, J.; Shao, Z.; Iris, Ç.; Pan, B.; Li, X.; Hu, Z.-T. A review of China's municipal solid waste (MSW) and comparison with international regions: Management and technologies in treatment and resource utilization. *J. Cleaner Prod.* **2021**, *293*, No. 126144.

(9) Wang, Y.; Shi, H.; Xia, T. D.; Zhang, T.; Feng, H. X. Fabrication and performances of microencapsulated paraffin composites with polymethylmethacrylate shell based on ultraviolet irradiation-initiated. *Mater. Chem. Phys.* **2012**, *135*, 181−187.

(10) Su, J.-F.; Wang, X.-Y.; Dong, H. Influence of temperature on the deformation behaviors of melamine−formaldehyde microcapsules containing phase change material. *Mater. Lett.* **2012**, *84*, 158−161.

(11) Şahan, N.; Paksoy, H. Determining influences of SiO2 encapsulation on thermal energy storage properties of different phase change materials. *Sol. Energy Mater. Sol. Cells* **2017**, *159*, 1−7.

(12) Chen, Z.; Cao, L.; Fang, G.; Shan, F. Synthesis and characterization of microencapsulated paraffin microcapsules as shape-stabilized thermal energy storage materials. *Nanoscale Microscale Thermophys. Eng.* **2013**, *17*, 112−123.

(13) Cao, L.; Tang, F.; Fang, G. Synthesis and characterization of microencapsulated paraffin with titanium dioxide shell as shape-stabilized thermal energy storage materials in buildings. *Energy Build.* **2014**, *72*, 31−37.

(14) Tang, B.; Qiu, M.; Zhang, S. Thermal conductivity enhancement of PEG/SiO_2 composite PCM by in situ Cu doping. *Sol. Energy Mater. Sol. Cells* **2012**, *105*, 242−248.

(15) Tang, B.; Wu, C.; Qiu, M.; Zhang, X.; Zhang, S. PEG/SiO2−Al2O3 hybrid form-stable phase change materials with enhanced thermal conductivity. *Mater. Chem. Phys.* **2014**, *144*, 162−167.

(16) Li, B.; Liu, T.; Hu, L.; Wang, Y.; Gao, L. Fabrication and properties of microencapsulated paraffin@SiO2 phase change composite for thermal energy storage. *ACS Sustainable Chem. Eng.* **2013**, *1*, 374−380.

(17) He, F.; Wang, X.; Wu, D. New approach for sol−gel synthesis of microencapsulated n-octadecane phase change material with silica wall using sodium silicate precursor. *Energy* **2014**, *67*, 223−233.
(18) Zhang, Y.; Tang, B.; Wang, L.; Lu, R.; Zhao, D.; Zhang, S. Novel hybrid form-stable polyether phase change materials with good fire resistance. *Energy Storage Mater.* **2017**, *6*, 46−52.
(19) Palacios, A.; De Gracia, A.; Haurie, L.; Cabeza, L.; Fernández, A.; Barreneche, C. Study of the thermal properties and the fire performance of flame retardant-organic PCM in bulk form. *Materials* **2018**, *11*, 117.
(20) Riddell, N.; van Bavel, B.; Ericson Jogsten, I.; McCrindle, R.; McAlees, A.; Chittim, B. Examination of technical mixtures of halogen-free phosphorus based flame retardants using multiple analytical techniques. *Chemosphere* **2017**, *176*, 333−341.
(21) Zhao, Q.; Chen, C.; Fan, R.; Yuan, Y.; Xing, Y.; Ma, X. Halogen-free flame-retardant rigid polyurethane foam with a nitrogen−phosphorus flame retardant. *J. Fire Sci.* **2017**, *35*, 99−117.
(22) Lallas, P. L. The stockholm convention on persistent organic pollutants. *Am. J. Int. Law* **2001**, *95*, 692−708.
(23) Shao, Y.; Ding, Y.; Dai, J.; Long, Y.; Hu, Z.-T. Synthesis of 5-hydroxymethylfurfural from dehydration of biomass-derived glucose and fructose using supported metal catalysts. *Green Synth. Catal.* **2021**, DOI: 10.1016/j.gresc.2021.01.006.
(24) Zhang, W.; He, X.; Song, T.; Jiao, Q.; Yang, R. The influence of the phosphorus-based flame retardant on the flame retardancy of the epoxy resins. *Polym. Degrad. Stab.* **2014**, *109*, 209−217.
(25) Cai, Y.; Wei, Q.; Huang, F.; Lin, S.; Chen, F.; Gao, W. Thermal stability, latent heat and flame retardant properties of the thermal energy storage phase change materials based on paraffin/high density polyethylene composites. *Renewable Energy* **2009**, *34*, 2117−2123.
(26) Velencoso, M. M.; Battig, A.; Markwart, J. C.; Schartel, B.; Wurm, F. R. Molecular firefighting—How modern phosphorus chemistry can help solve the challenge of flame retardancy. *Angew. Chem., Int. Ed.* **2018**, *57*, 10450−10467.
(27) Wirasaputra, A.; Yao, X.; Zhu, Y.; Liu, S.; Yuan, Y.; Zhao, J.; Fu, Y. Flame-retarded epoxy resins with a curing agent of DOPO-triazine based anhydride. *Macromol. Mater. Eng.* **2016**, *301*, 982−991.
(28) Yang, S.; Zhang, Q.; Hu, Y. Synthesis of a novel flame retardant containing phosphorus, nitrogen and boron and its application in flame-retardant epoxy resin. *Polym. Degrad. Stab.* **2016**, *133*, 358−366.
(29) Wu, G.; An, J.; Sun, D.; Tang, X.; Xiang, Y.; Yang, J. Robust microcapsules with polyurea/silica hybrid shell for one-part self-healing anticorrosion coatings. *J. Mater. Chem. A* **2014**, *2*, 11614−11620.
(30) Wu, G.; An, J.; Tang, X.-Z.; Xiang, Y.; Yang, J. A versatile approach towards multifunctional robust microcapsules with tunable, restorable, and solvent-proof superhydrophobicity for self-healing and self-cleaning coatings. *Adv. Funct. Mater.* **2014**, *24*, 6751−6761.
(31) Sanghvi, S. P.; Nairn, J. G. Effect of viscosity and interfacial tension on particle size of cellulose acetate trimellitate microspheres. *J. Microencapsulation* **1991**, *9*, 215−227.
(32) Park, S.-J.; Kim, K.-S.; Kim, S.-H. Effect of poly(ethylene oxide) on the release behaviors of poly(ε-caprolactone) microcapsules containing erythromycin. *Colloids Surf., B* **2005**, *43*, 238−244.
(33) Zhang, H.; Wang, X. Fabrication and performances of microencapsulated phase change materials based on n-octadecane core and resorcinol-modified melamine−formaldehyde shell. *Colloids Surf., A* **2009**, *332*, 129−138.
(34) Zhang, H.; Wang, X.; Wu, D. Silica encapsulation of n-octadecane via sol−gel process: A novel microencapsulated phase-change material with enhanced thermal conductivity and performance. *J. Colloid Interface Sci.* **2010**, *343*, 246−255.
(35) Hu, Z.-T.; Liu, J.-W.; Zhao, J.; Ding, Y.; Jin, Z.; Chen, J.; Dai, Q.; Pan, B.; Chen, Z.; Chen, J. Enhanced BiFeO3/Bi2Fe4O9/H2O2 heterogeneous system for sulfamethoxazole decontamination: System optimization and degradation pathways. *J. Colloid Interface Sci.* **2020**, *577*, 54−65.
(36) Shi, C.; Jing, Y.; Jia, Y. Solvent extraction of lithium ions by tri-n-butyl phosphate using a room temperature ionic liquid. *J. Mol. Liq.* **2016**, *215*, 640−646.
(37) Haghshenas Fatmehsari, D.; Darvishi, D.; Etemadi, S.; Eivazi Hollagh, A. R.; Keshavarz Alamdari, E.; Salardini, A. A. Interaction between TBP and D2EHPA during Zn, Cd, Mn, Cu, Co and Ni solvent extraction: A thermodynamic and empirical approach. *Hydrometallurgy* **2009**, *98*, 143−147.
(38) Zhang, H.; Pang, H.; Zhang, L.; Chen, X.; Liao, B. Biodegradability of polyurethane foam from liquefied wood based polyols. *J. Polym. Environ.* **2013**, *21*, 329−334.
(39) Cai, Y.; Hu, Y.; Song, L.; Kong, Q.; Yang, R.; Zhang, Y.; Chen, Z.; Fan, W. Preparation and flammability of high density polyethylene/paraffin/organophilic montmorillonite hybrids as a form stable phase change material. *Energy Convers. Manage.* **2007**, *48*, 462−469.
(40) Liang, S.; Neisius, M.; Mispreuve, H.; Naescher, R.; Gaan, S. Flame retardancy and thermal decomposition of flexible polyurethane foams: Structural influence of organophosphorus compounds. *Polym. Degrad. Stab.* **2012**, *97*, 2428−2440.
(41) Shi, Y.; Yu, B.; Duan, L.; Gui, Z.; Wang, B.; Hu, Y.; Yuen, R. K. K. Graphitic carbon nitride/phosphorus-rich aluminum phosphinates hybrids as smoke suppressants and flame retardants for polystyrene. *J. Hazard. Mater.* **2017**, *332*, 87−96.
(42) Yemisci, F.; Yesil, S.; Aytac, A. Improvement of the flame retardancy of plasticized poly (lactic acid) by means of phosphorus-based flame retardant fillers. *Fire Mater.* **2017**, *41*, 964−972.
(43) Lyon, R. E.; Walters, R. N. Pyrolysis combustion flow calorimetry. *J. Anal. Appl. Pyrolysis* **2004**, *71*, 27−46.
(44) Jiao, C.; Wang, H.; Li, S.; Chen, X. Fire hazard reduction of hollow glass microspheres in thermoplastic polyurethane composites. *J. Hazard. Mater.* **2017**, *332*, 176−184.
(45) Vigouroux, C.; Stavrakou, T.; Whaley, C.; Dils, B.; Duflot, V.; Hermans, C.; Kumps, N.; Metzger, J. M.; Scolas, F.; Vanhaelewyn, G.; Muller, J. F.; Jones, D. B. A.; Li, Q.; De Maziere, M. FTIR time-series of biomass burning products (HCN, C2H6, C2H2, CH3OH, and HCOOH) at Reunion Island (21 degrees S, 55 degrees E) and comparisons with model data. *Atmos. Chem. Phys.* **2012**, *12*, 10367−10385.
(46) Lafleur, A. L.; Gagel, J. J.; Longwell, J. P.; Monchamp, P. A. Identification of aromatic alkynes and acyclic polyunsaturated hydrocarbons in the output of a jet-stirred combustor. *Energy Fuels* **1988**, *2*, 709−716.

https://doi.org/10.1021/acs.langmuir.0c03587
Langmuir 2021, 37, 6380−6387